

Simulation of Inspiratory Airflow in Stenotic Trachea and its Effect on Mainstem Bifurcation

Ayodele J. Oyejide^{1*}, Joy E. Onuh², Emmanuel D. Ephraim² and Adetokunbo A. Awonusi^{2#}

^{1,2}Researchers, Department of Biomedical Engineering, University of Ibadan, Oyo, Nigeria

^{2#}Researcher, Department of Mechanical Engineering, University of Ibadan, Oyo, Nigeria

DOI: [10.36348/sjbr.2021.v06i11.002](https://doi.org/10.36348/sjbr.2021.v06i11.002)

| Received: 03.10.2021 | Accepted: 08.11.2021 | Published: 18.11.2021

*Corresponding author: Ayodele James Oyejide

Abstract

Background: Tracheal stenosis is a narrowing condition of the trachea that can lead to life threatening breathing complications depending on the extent of reduction in the airway diameter. This condition affects not just the lung's performance to draw air during inspiration but also the flow behavior in the bronchi generations. **Methods:** Computational simulations were performed in idealistic healthy and stenosed tracheobronchial models of adult and infant airways consisting of the trachea and mainstem bronchi alone. Effect of 70% reduction in trachea diameter was investigated for both models using Ansys Fluent. **Results:** We realized that while airflow developed along the center in the healthy model, flow in the stenosed tracheae moved in a jet-like manner, forcing its way across the airway tract with velocity 5 m/s greater than that in the healthy airways. This high jet-like flow at the center in the stenosed tracheae led to high flow impact at the bronchi bifurcation. Consequently, wall shear stress at the bifurcation was high in both stenosis cases. **Conclusion:** This study shows that tracheal stenosis potentially leads to high flow impact and wall shear stress at the bifurcation of mainstem bronchi, and this effect will have severe consequences in infants than adults.

Key words: Tracheal Stenosis, Mainstem Bronchi, Bifurcation, Inspiratory flow, Wall Shear Stress (WSS).

Copyright © 2021 The Author(s): This is an open-access article distributed under the terms of the Creative Commons Attribution 4.0 International License (CC BY-NC 4.0) which permits unrestricted use, distribution, and reproduction in any medium for non-commercial use provided the original author and source are credited.

INTRODUCTION

Several health conditions such as malformation of cartilage, scar tissue formation, or genetic disorders can lead to narrowing of the trachea, popularly referred to as the windpipe [1]. It is estimated from clinical studies that while it is possible not to develop breathing challenges if narrowing is minimal, a significant narrowing of more than 50%, particularly 70-90%, will cause respiratory disorder if left untreated [2]. Tracheal stenosis, like stenosis in other generation of the respiratory tracheobronchial airway, causes airflow resistance that alters flow dynamics. Consequently, studies have been carried out to analyze the flow phenomenon in tracheal stenosis by utilizing idealistic and realistic models. Mark Brouns *et al.*, [3] studied the flow dynamics in a critical tracheal stenosis with different degree of constrictions using computational fluid dynamics; they focused on studying the flow pattern and the pressure drop. Their study shows that overall pressure drop at rest is only affected by critical degree of stenosis. Stapleton *et al.*, [4] also tried to investigate if flow as low as 3l/min in a stenosed trachea would alter the flow pattern through

the upper airway. They realized that air flow at such low velocity could result in turbulence flow behavior due to local structural complexity in the geometry.

Recently, Limin Zhu *et al.*, [5] studied the flow dynamics in multi-segmental complex congenital tracheal stenosis using computational fluid dynamics. They found out that the multi-stage constriction affected the aerodynamics parameter, which shows turbulence flow downstream of the tracheal stenosis and upstream of the bronchi. In a study by Mimouni-Benabu *et al.*, [6] using steady calculations to evaluate flow dynamics in stenosed trachea of different age groups, they found out that pressure drop was greatly influenced by age. This study was validated by clinical measurement of pressure drop. Many other studies have taken advantage of computational fluid dynamics coupled with realistic and/ idealized geometry to study the impact of tracheal stenosis on the flow behavior in the tracheobronchial airway, particularly the mainstem bronchi [7-10]. The computational fluid dynamics variables derived from these studies, such as the airflow velocity, wall pressure, pressure drop, and wall shear stress have proven that stenosis influences the breathing

condition in both inspiratory and expiratory processes [11, 12], which may affect patients depending on age, previous medical conditions and life style [2].

The objective of this study is to provide a distinct description of airflow behavior in tracheal stenosis with 70% constriction, and to evaluate the effect of this flow nature on the bifurcation of the mainstem bronchi of idealized infant and adult tracheobronchial airways consisting of generation 0 to 1. This study focuses on providing a simplified computational analysis to enhance understanding of airflow dynamics in tracheal stenosis and the effect on mainstem bronchi, in order to develop the best treatment models and strategies.

METHODS

Geometry

Table 1 shows the geometry parameter used in this study. The models are idealized 3D human

tracheobronchial airway (generation 0-1) based on Weibel [13] model. The geometry is constructed with varying diameter from the inlet (the trachea) to the outlets (the mainstem bronchi). The angle of bifurcation of the bronchi from the trachea is 70 degrees and the right bronchus is slightly larger than the left bronchus. The bronchi were truncated at the same length, which would not affect the result since the mainstem bronchi bifurcation is of more interest concern in this study. Basically, two different models were constructed for two cases: a healthy and a stenosed trachea tracheobronchial airway model for infant and adult. The 3D model parameter was adopted from the proposed model of Florens *et al.*, [14] and Lin and Goodarz [15]. The narrowing at the trachea in all stenosis models is 70% and it occurs along the center of the entire trachea length. The different geometries are shown below in table 1 where LB and RB represent the left and right main bronchi, respectively.

Table-1: Geometry of the idealized model consisting of the trachea and bronchi

Airway Model	Length (m)	Diameter (m)	Curvature radius (m)	Angle of bifurcation
Tracheal	0.08	0.02	0.0016	-
LB	0.04	0.014	0.0752	70 ⁰
RB	0.04	0.013	0.0455	70 ⁰

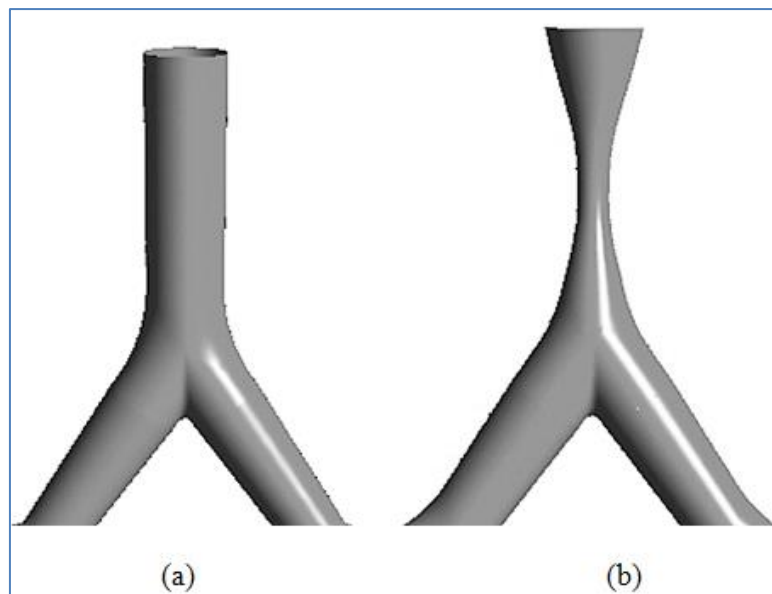


Fig-1: Schematic view of truncated idealized (a) healthy and (b) stenosed tracheobronchial airway models with 70 % narrowing of the trachea airway

Meshing

On importing the 3D geometry into Ansys Inc. software, inflation criteria were selected on the circular faces and the mesh was generated after selecting

unstructured tetrahedral cells on the entire airway models. A grid cells of >1700000; maximum skewness < 0.87; minimum orthogonal quality > 0.125 were selected after the grid dependence examination.

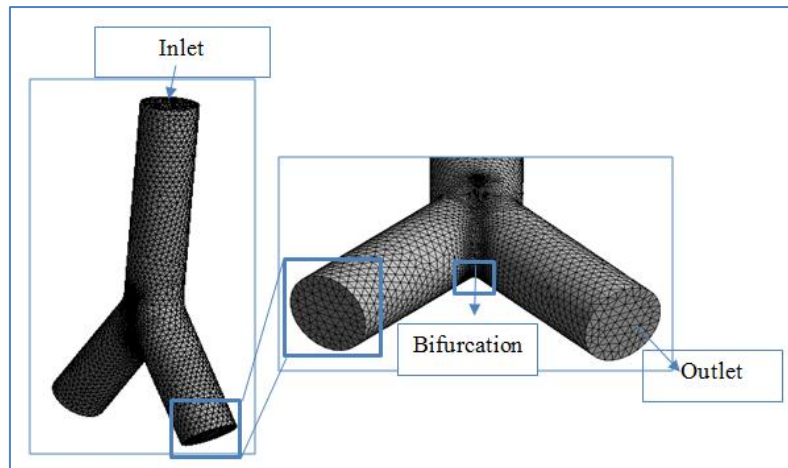


Fig-2: Grid distribution in enlarged 3D model of the control (healthy) tracheobronchial airway with emphasis on the inlet, bifurcation, and outlet region.

Assumptions and Boundary Conditions

The tracheobronchial airway is assumed rigid as shown in figure 1. The conducting material is air, flowing into the trachea at steady flow rate. Hence, the fluid in this study is considered laminar incompressible fluid. In addition, there is no velocity at the wall hence, no slip during fluid motion. The driving force at the inlet and outlet are velocity and pressure, respectively. The inspiratory flow rates and inlet velocities for the infant and adult models are 0.059 l/s and 1.16 m/s and 0.315 l/s and 0.80 m/s, respectively, adopted from the numerical respiratory simulations of Tsage [16].

Numerical Methods

The CFD computation was performed on ANSYS Fluent. The governing equations for the incompressible fluid are continuity and momentum equations, which in the simplest form are written as:

$$\nabla \cdot \mathbf{v} = 0 \quad (1)$$

$$\rho (\mathbf{v} \cdot \nabla \mathbf{v}) = -\nabla p + \mu \nabla^2 \mathbf{v} \quad (2)$$

The finite-volume based CFD technique was used to solve the continuity and momentum governing equations (Eqn. 1 and 2). Table 2 summarizes the iteration and solver parameters used for setting the simulation conditions.

Table-2: CFD parameter for numerical simulation of airflow in the models

Parameter	ANSYS Fluent
Solver type	Pressure-based
Solution algorithm	SIMPLE
Discretization scheme (Pressure term)	Second order
Discretization scheme (Momentum terms)	Second order upwind
Under relaxation factor (Pressure)	0.2
Under relaxation factor (Momentum)	0.5
Residual (Convergence criteria)	$< 10^{-5}$
Density (ρ)	1.225 kg/m ³
Viscosity (μ)	1.7894 x 10 ⁻⁵ kg/Ms
Womersley number	0.44

RESULT AND DISCUSSION

In this section, the simulation results for inspiratory flow in the stenosed and normal tracheobronchial airways are presented. The computational variables of interest are the airflow velocity at the trachea, the magnitude of airflow at the bifurcation, and the wall shear stress (WSS) resulting from such flow magnitude at the bifurcation. A total of 8 simulations (2 steady state for inspiratory flow velocity and 2 for wall shear stress in each case) were performed in both airway models of the two different age groups under consideration. The flow streamlines

are also presented in this section to give vivid representation of flow behavior at the bifurcation in the stenosed airway models. In addition, the simulation charts presented in this section for both infant and adult airway models are not according to scale; they have been expanded to make the presentation clearer while retaining the exact values gotten from the computations. Also, the derived values for maximum inspiratory airflow velocity and wall shear stress at the stenosis and bifurcation regions in the infant and adult airway models are presented in table 3 and 4, respectively.

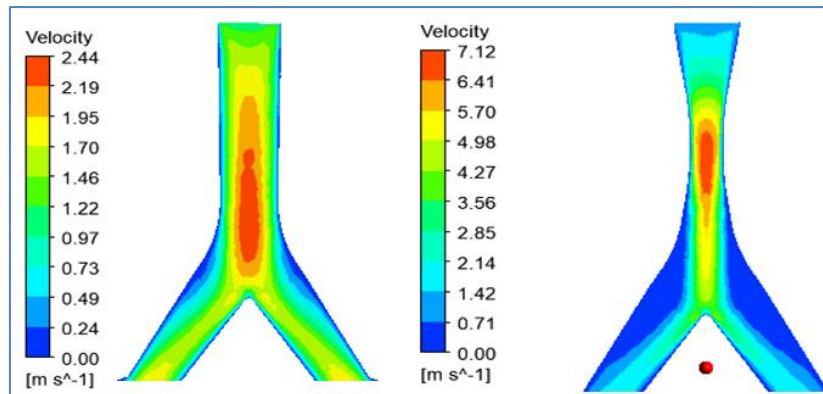


Fig-3: Velocity contour at mid-plane in healthy tracheobronchial (left) and 70% narrowed trachea (right) for a developing infant idealized airway model at flow rate of 0.059l/s.

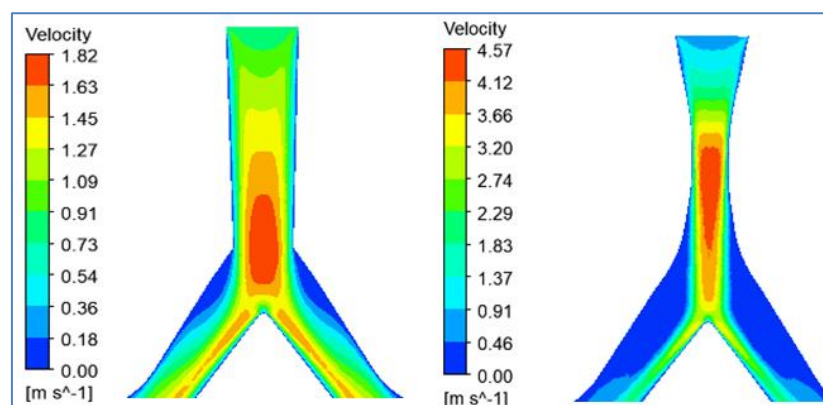


Fig-4: Velocity contour at mid-plane in healthy tracheobronchial (left) and 70% narrowed trachea (right) for an idealized adult airway model at flow rate of 0.315 l/s.

Flow velocity, Streamlines and Wall Shear Stress in Infant Airway Model

Figure 3 shows the flow velocity in the healthy (left) and stenosed (right) airway models for infant. In the healthy trachea airway, the flow is seen to develop at the center with maximum flow velocity of 2.44 m/s, about twice the entry flow rate of 1.16 m/s that was computed. This implies a smooth transition of airflow from the trachea into the main bronchi and ultimately into the lower tracheobronchial terminals. Furthermore, the healthy airflow distribution from the trachea to the mainstem bronchi resulted in relatively minimal stress at the bifurcation, with maximum flow impact value of the range of 1.70 -1.95 m/s.

On the other hand, the flow behavior in the stenosed trachea is obviously unique, as a jet-like flow develops towards the center of the region of constriction with the protruding edge facing the point of bifurcation. The jet-like air forces its way out with maximum velocity of 7.12 m/s, which is about 5.68m/s greater in magnitude when compared to maximum flow in the healthy model. However, the high flow velocity in the stenosed trachea model does not correspond to healthy flow because the flow occurs at the center of the mid cross section, implying that the flow speed needed to increase in order to overcome the high resistance. Obviously, the jet velocity dropped immediately the

flow developed away from the narrowed region to a value of about 5.70 m/s; though still about 3.26 m/s greater than the maximum flow in the healthy airways.

Although the flow behavior seems to be uniform at the bifurcation in both the healthy and stenosed models, the magnitude of flow hitting the exact point of bifurcation in the deformed airway model was greater, with a value of about 4.27 m/s while the value in the healthy model was about 1.95 m/s. The high value of flow hitting the point of bifurcation in the stenosed trachea model indicates a potential medical threat [17]. This is obvious from the wall share stress behavior and value at the bifurcation of the same airway model, where the WSS reaches a value of 3.60 Pa (see figure 6 and table 4). This high value can lead to damage on the airway tract over time if not given clinical attention. A reasonable range of WSS acted at the bifurcation in the healthy airway model, with a value of 1.21 Pa (see figure 6 and table 4). According to Kittisak and Ramana [18], this is a healthy range of stress for the region.

Figure 5 shows clearer illustration of the flow pattern in both models of the infant airway. From the velocity streamlines in 5a, it is observed that the lines converged smoothly at and away from the bifurcation in the healthy model, while in the stenosed airway model,

the lines split randomly at the bifurcation. This flow behavior is expected, since the air moves out of the constricted region with high velocity towards the center. As air pulls out and hits the bifurcation, the

underdeveloped flow is distributed in an oscillatory manner before moving down the bronchi, developing along the way.

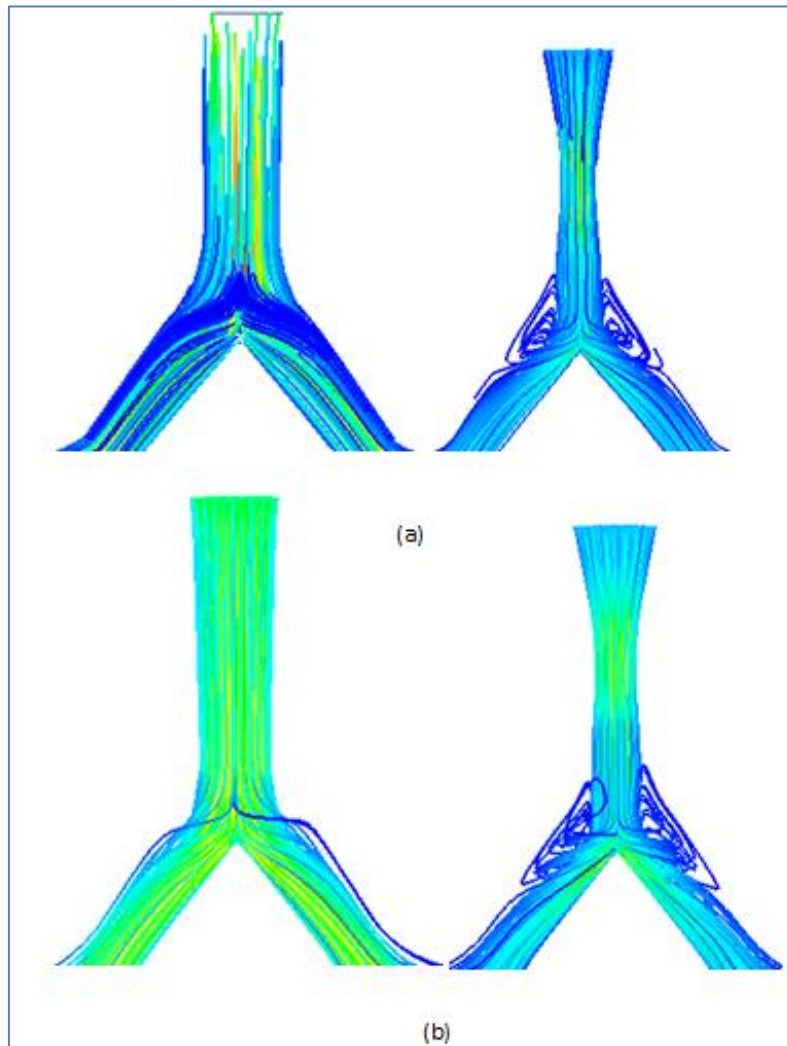


Fig-5: Airflow streamlines in (a) infant and (b) adult for healthy (left) and stenosed (right), depicting the flow distribution at the bifurcations

Flow velocity, Streamlines and Wall Shear Stress in Adult Airway Model

If the values of the geometry were to be increased, say for adult airway; using geometry parameters of idealistic adult airway from Ou *et al.*, [19] and Tsega [16], at flow rate of 0.315 l/s and inspiratory velocity of 0.80 m/s, the maximum velocities in the healthy and diseased airway models were 1.82 m/s and 4.57 m/s, respectively (see figure 4). The flow in the healthy trachea model is fully developed, almost occupying the entire airway. In the

stenosed airway model, the maximum velocity occurs at the center of the airway in the same pattern as in the infant airway expect that the magnitude is higher in the infant airway, with approximately 2.89 m/s. Despite the increase in the adult airway diameter and 70% constriction in both age group airway models, the velocity of airflow in the stenosed trachea in infant was higher, confirming the literature [16, 20] that airflow characteristic decline as humans grow from infant to child and to adult.

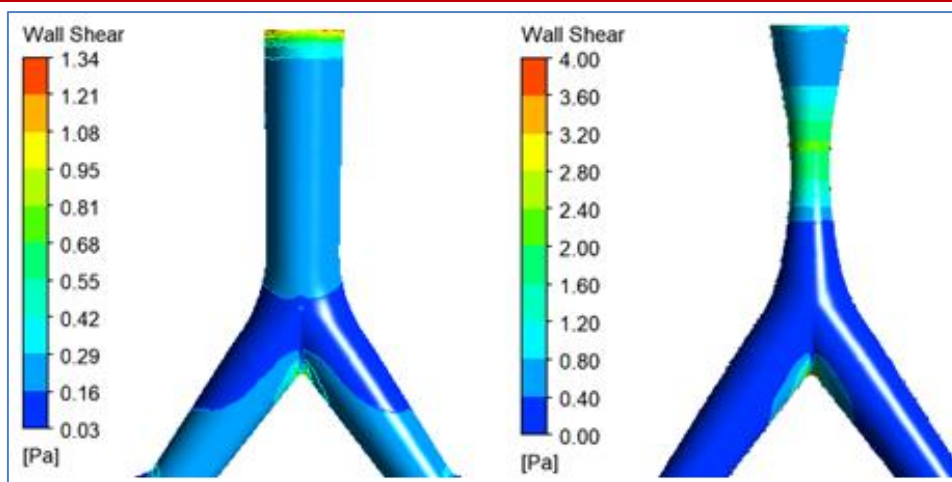


Fig-6: Wall shear stress distribution at the walls of the idealized infant tracheobronchial airway models for (left) healthy and (right) deformed trachea.

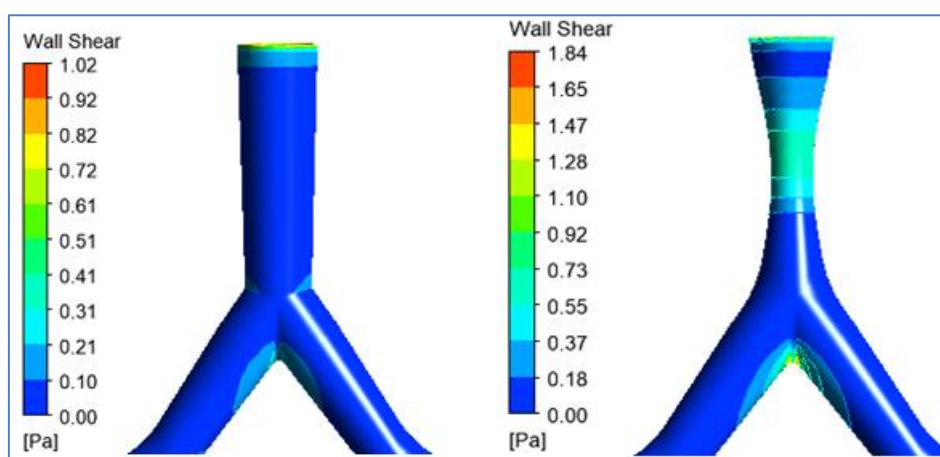


Fig-7: Wall shear stress distribution at the walls of the idealized adult tracheobronchial airway models for (left) healthy and (right) deformed trachea.

Table-3: Inspiratory velocity values at the trachea and magnitude of impact on the bifurcation for both models under consideration

Inspiratory Velocity (m/s)	Healthy Trachea	Bifurcation	Stenosed trachea	Bifurcation
Infant	2.19-2.44	1.70-1.95	6.41-7.12	4.27- 4.98
Adult	1.63-1.82	1.45-1.63	4.12-4.57	3.20-3.66

Table-4: Inspiratory wall shear stress values at the trachea and bifurcation for both models under consideration

Inspiratory WSS (Pa)	Healthy Trachea	Bifurcation	Stenosed trachea	Bifurcation
Adult	0.10	0.31	0.92	1.65
Infant	0.29	1.21	2.80	3.60

As shown in figure 4, the narrowed flow jet in the stenosed adult airway is almost hitting the point of bifurcation at high magnitude of 3.66 m/s. The corresponding value in the healthy airway model is about 1.63 m/s; a difference of 2.03 m/s. This difference in magnitude had substantial impact on the wall shear stress behavior at the bifurcating region in both airway models. The maximum WSS at the bifurcation in the healthy and stenosed tracheobronchial adult models

were 0.31 Pa and 1.65 Pa (see figure 7), respectively. Interestingly, despite the high magnitude of flow hitting the bifurcating region in the adult airway model, the effect of WSS was higher in the infant airway model (see table 4). Possibly, this characteristic is due to the sensitivity of the infant developing airways, implying that in more developed airways, such as in child and adult, the effect of wall shear stress (WSS) resulting from stenosis may be less severe when compared to that

of infants. The streamline pattern in the adult airway model follows the same pattern as in the infant model for both healthy and stenosed airways. However, in the healthy adult airway, there is slight splitting at the bifurcation down into the bronchi. We can infer that even for healthy trachea, air flow more uniformly in the infant airways than in the adult airways, probably due to aging factors.

CONCLUSION

In this study, computational fluid simulation was carried out in an idealistic model of adult and infant tracheobronchial airways consisting of the trachea and mainstem bronchi. The CFD variable of interest was the flow velocity in the stenosed tracheae and how the flow dynamics of such narrowing affects the magnitude of air that hits the bifurcation. By comparison, airflow in the healthy adult airway model developed towards the center and moves at steady velocity. This flow behavior led to relatively low value of wall shear stress at the bifurcation. However, the flow magnitude in the stenosed airway model is 5.68 m/s greater than in the healthy and it moves in a jet manner, forcing it way towards the center to overcome the constriction. This, in essence, resulted to high wall shear stress both on the tract and at the bifurcation. Accordingly, in the airway model of infant, the flow velocity follows same pattern as in the adult airway model except that the value of wall shear stress at the bifurcation in infant is greater than in adult airway model. Hence, it can be inferred from this study that the bifurcating region of the mainstem bronchi is greatly influenced by stenosis at the trachea. Respiratory diseases that reduce the trachea airway by more than half the anatomical diameter will not only resist flow, but will also lead to high flow impact on the immediate bifurcation. The outcome also reveals that the flow behavior in diseased trachea is similar whether in developed adult airways or in developing infant airways.

Disclosure of conflict of interest

The authors declare that there is no conflict of interest.

REFERENCE

- Copploe, A., Vatani, M., Choi, J. W., & Tavana, H. (2019). A Three-Dimensional Model of Human Lung Airway Tree to Study Therapeutics Delivery in the Lungs. *Annals of biomedical engineering*, 47(6), 1435-1445.
- Raman, T., Chatterjee, K., Alzghoul, B. N., Innabi, A. A., Tulunay, O., Bartter, T., & Meena, N. K. (2017). A bronchoscopic approach to benign subglottic stenosis. *SAGE open medical case reports*, 5, 2050313X17713151.
- Brouns, M., Jayaraju, S. T., Lacor, C., De Mey, J., Noppen, M., Vincken, W., & Verbanck, S. (2007). Tracheal stenosis: a flow dynamics study. *Journal of Applied Physiology*, 102(3), 1178-1184.
- Stapleton, K. W., Guentsch, E., Hoskinson, M. K., & Finlay, W. H. (2000). On the suitability of $k-\epsilon$ turbulence modeling for aerosol deposition in the mouth and throat: a comparison with experiment. *Journal of Aerosol Science*, 31(6), 739-749.
- Zhu, L., Gong, X., Liu, J., Li, Y., Zhong, Y., Shen, J., & Xu, Z. (2020). Computational evaluation of surgical design for multisegmental complex congenital tracheal stenosis. *BioMed research international*, 2020.
- Mimouni-Benabu, O., Meister, L., Giordano, J., Fayoux, P., Loundon, N., Triglia, J. M., & Nicollas, R. (2012). A preliminary study of computer assisted evaluation of congenital tracheal stenosis: A new tool for surgical decision-making. *International journal of pediatric otorhinolaryngology*, 76(11), 1552-1557.
- Qi, S., Li, Z., Yue, Y., van Triest, H. J., & Kang, Y. (2014). Computational fluid dynamics simulation of airflow in the trachea and main bronchi for the subjects with left pulmonary artery sling. *Biomedical engineering online*, 13(1), 1-15.
- Zhu, L., Shen, J., Gong, X., Liu, L., Liu, J., & Xu, Z. (2019, July). Effects of different modes of mechanical ventilation on aerodynamics of the patient-specific airway: A numerical study. In *2019 41st Annual International Conference of the IEEE Engineering in Medicine and Biology Society (EMBC)* (pp. 4961-4964). IEEE.
- Shen, J., Zhu, L., Tong, Z., Liu, J., Umezu, M., Xu, Z., & Liu, J. (2017). Surgical timing prediction of patient-specific congenital tracheal stenosis with bridging bronchus by using computational aerodynamics. In *Advanced Computational Methods in Life System Modeling and Simulation* (pp. 181-190). Springer, Singapore.
- Ho, C. Y., Liao, H. M., Tu, C. Y., Huang, C. Y., Shih, C. M., Su, M. Y. L., ... & Shih, T. C. (2012). Numerical analysis of airflow alteration in central airways following tracheobronchial stent placement. *Experimental hematology & oncology*, 1(1), 1-8.
- Zhu, L. M., Gong, X. L., Shen, J. Y., Liu, L. P., Liu, J. F., Liu, J. L., & Xu, Z. M. (2019). Application of computational aerodynamics on the risk prediction of PM2. 5 in congenital tracheal stenosis. In *World Congress on Medical Physics and Biomedical Engineering 2018* (pp. 807-811). Springer, Singapore.
- Zhu, L., Liu, J., Zhang, W., Sun, Q., Hong, H., Du, Z., ... & Umezu, M. (2015, May). Computational aerodynamics of long segment congenital tracheal stenosis with bridging bronchus. In *2015 10th Asian Control Conference (ASCC)* (pp. 1-5). IEEE.
- Weibel, E. R. (1963). *Morphometry of the Human Lung*, Academic Press, New York, NY, USA
- Florens, M., Sapoval, B., & Filoche, M. (2011). An anatomical and functional model of the human

- tracheobronchial tree. *Journal of Applied Physiology*, 110(3), 756-763.
15. Tian, L., & Ahmadi, G. (2012). Transport and deposition of micro-and nano-particles in human tracheobronchial tree by an asymmetric multi-level bifurcation model. *The Journal of Computational Multiphase Flows*, 4(2), 159-182.
 16. Tsega, E. G. (2018). Computational fluid dynamics modeling of respiratory airflow in tracheobronchial airways of infant, child, and adult. *Computational and mathematical methods in medicine*, 2018.
 17. Green, A. S. (2004). Modelling of peak-flow wall shear stress in major airways of the lung. *Journal of biomechanics*, 37(5), 661-667.
 18. Koombua, K., & Pidaparti, R. M. (2008). Inhalation induced stresses and flow characteristics in human airways through fluid-structure interaction analysis. *Modelling and Simulation in Engineering*, 2008.
 19. Ou, C., Li, Y., Wei, J., Yen, H. L., & Deng, Q. (2017). Numerical modeling of particle deposition in ferret airways: A comparison with humans. *Aerosol Science and Technology*, 51(4), 477-487.
 20. Oakes, J. M., Roth, S. C., & Shadden, S. C. (2018). Airflow simulations in infant, child, and adult pulmonary conducting airways. *Annals of biomedical engineering*, 46(3), 498-512.